JSS Focus Issue on Advanced Interconnects: Materials, Processing, and Reliability

Chemically Amplified, Positive Tone, Polynorbornene Dielectric for Microelectronics Packaging

Brennen K. Mueller,[a,*] Jared M. Schwartz,[a,*] Alexandra E. Sutlief,[a] William K. Bell,[b] Colin O. Hayes,[b] Edmund Elce,[c] C. Grant Willson,[b] and Paul A. Kohl[a,,z]**

[a]*School of Chemical and Biomolecular Engineering, Georgia Institute of Technology, Atlanta, Georgia 30332-0100, USA*
[b]*Department of Chemistry, The University of Texas at Austin, Austin, Texas 78712-1224, USA*
[c]*Promerus LLC, Brecksville, Ohio 44141, USA*

A low permittivity, positive tone, polynorbornene dielectric has been developed that exhibits excellent lithographic and electrical properties. The polymer resin is a random copolymer of a norbornene hexafluoroalcohol (NBHFA) and a norbornene tert-butyl ester (NBTBE). High optical sensitivity and contrast were achieved using a chemically amplified solubility switching mechanism through the acid-catalyzed deprotection of the tert-butyl ester functionality. After developing in aqueous base, the film was thermally cured through a Fischer esterification reaction, resulting in a cross-linked permanent dielectric. The effect of the photoacid generator (PAG) concentration on the lithographic patterning and curing reactions was studied. Higher PAG loading was favorable for both sensitivity and dielectric constant. The sensitivity of a formulation was measured as low as 8.09 mJ/cm^2. The molar ratio of the two monomers composing the polymer was varied. A higher NBHFA content was favorable because it resulted in a lower modulus, lower shrinkage, and lower dielectric constant and loss. A formulation with 70 mol% of the NBHFA had a modulus of 2.60 GPa, a 12.2% volume decrease during cure, and a dielectric constant of 2.23. The direction-dependent coefficient of thermal expansion was measured, and it was found that the anisotropy of the PNB films decreased with higher NBTBE content.
 [DOI: 10.1149/2.0011501jss]

Manuscript received June 13, 2014. Published August 4, 2014. This was Paper 1471 presented at the Orlando, Florida, Meeting of the Society, May 11–15, 2014. *This paper is part of the JSS Focus Issue on Advanced Interconnects: Materials, Processing, and Reliability.*

Permanent dielectric materials are used in microelectronic devices and packages to separate and insulate components and interconnect. Low dielectric constant (low-k) insulators are desirable for on-chip, chip-to-chip, chip-to-package, and on-package wiring to avoid electrical delay and lower the energy consumed in the signal interconnect.[1–3] Polymers are widely used for these purposes because they offer a low-stress, easily processed alternative to inorganic dielectrics.[2–5] In addition, photosensitive dielectrics are desirable because they can be directly patterned by photolithographic means. Lithographically printed dielectrics do not require the use of photoresist or additional pattern transfer steps, which can be costly and expose the device to aggressive wet or dry etch process steps.

Positive tone dielectrics are especially attractive because they result in sloped sidewalls that are generally favored for void-free electroplating of copper. Positive tone materials also exhibit better process yield because exposures through dark-field masks are less susceptible to particle defects. The ability to develop the latent image in an aqueous base developer mitigates the need for environmentally unfriendly organic solvent developers. High sensitivity is very important since it directly leads to higher throughput and tool utilization since less optical energy is required for the solubility switching reaction. The sensitivity of the photopatternable material is coupled to the quantum efficiency of the photoactive compound. Poor quantum efficiency often requires a high loading of the photoactive compounds to effect the inhibition or solubility switch, which limits the thickness of the film that can be exposed. High contrast is very desirable for achieving high aspect ratio, densely packed features.

Once patterned, permanent dielectrics are generally cured (C-staged) or at least partially cured (B-staged) to achieve good thermo-mechanical and electrical properties. Several process-related, physical properties are important for cured dielectric materials including thermal stability, glass transition temperature (T_g), cure temperature, volume change during cure, coefficient of thermal expansion (CTE), elastic modulus, hardness, toughness, and complex permittivity.[6] Each of these properties can have a different weighting in terms of importance depending on the specific application.

Current positive tone, permanent dielectric polymers use diazonaphthoquinone-based (DNQ) photochemistry, which provides relatively low sensitivity (D_{100} > 300 mJ/cm^2) and low contrast (< 2.5).[7–9] To inhibit the dissolution in the developer, the DNQ is added at relatively large concentrations, typically 15 to 30 mass parts per 100 mass parts polymer (pphr) to the original mixture. In cases where DNQ does not interact with the resin through hydrogen bonding, contrast is achieved purely through the dissolution rate difference between the exposed and unexposed regions. Erosion of the unexposed regions (i.e. dark erosion) during the develop step is an issue because any loss of the unexposed material reduces the overall thickness of the final polymer film. The sensitivity of DNQ-loaded films is also limited by the absorbance of these films along with the low quantum efficiency of DNQ.[10] High optical absorbance leads to the need for a high optical dose in order to fully expose the photoactive compound deep in the film.

An alternative photochemistry to DNQ is chemical amplification (CA).[11,12] In the case of CA, pendent protected carboxylic acids or acidic alcohols are incorporated onto the base polymer making the polymer initially insoluble in aqueous base. A photoacid generator (PAG) is added to the formulation, and upon exposure, a strong acid is created which catalyzes the deprotection reaction resulting in formation of the carboxylic acid or alcohol. The chemical protection is often achieved by using carboxylic acid or alcohol moieties protected with a tert-butyl group to yield a tert-butyl ester, or tert-butoxycarbonyl (t-BOC) group, respectively. Deprotection of the tert-butyl ester with the acid catalyst generates isobutylene vapors that diffuse out of the film and contributes to a volume change in the film during patterning. After deprotection of the protected acid or alcohol, the aqueous base developer can deprotonate the carboxylic acid or alcohol and water can coordinate with the carboxyl or alkoxy anion to dissolve the film. Since the deprotection reaction is catalyzed by the photoacid, only a small loading of PAG is required for patterning, so the overall absorbance of the film remains low. Previously, the chemically amplified

*Electrochemical Society Student Member.
**Electrochemical Society Fellow.
zE-mail: kohl@gatech.edu

photochemistry had not been used to pattern permanent materials because of the difficulty in cross-linking the final product. While other cross-linking mechanisms can be considered, some are not compatible with the photogenerated acid, such as the epoxy ring-opening reaction, because the photogenerated acid could initiate cross-linking in competition with the photopatterning.

The functional chemistry for a chemically amplified, cross-linkable polymer has recently been demonstrated with a copolymer of tert-butyl methacrylate and 2-hydroxyethyl methacryate.[13] The solubility switch was achieved by acid catalyzed deprotection of the tert-butyl ester to form an aqueous base soluble carboxylic acid. Formulations with 1 and 3 pphr PAG were found to have a contrast between 12.7 and 5.2, respectively. The sensitivity, as measured by the D_{100}, was found to be 50.2 and 32.2 mJ/cm^2 for the 1 and 3 pphr PAG, respectively. This material was cross-linked via a Fischer esterification reaction between the pendent carboxylic acid and alcohol groups. In this case, the cross-linking reaction was much slower than the deprotection reaction, so the cross-linking did not interfere with photo-patterning. Cross-linking was shown by measuring changes in residual stress and solubility of the final film. Although this polymer demonstrated the CA concept for a cross-linkable polymer, the thermal stability of polymethacrylates is not sufficiently high for some applications, such as the thermal stability for solder reflow to 265°C.[14]

In this study, a chemically amplified, aqueous developable, cross-linkable chemistry is demonstrated using a polynorbornene (PNB) backbone. The PNB backbone has been shown to have excellent thermal stability and electrical properties. The polymer using the PNB backbone has excellent solubility in the developer and adhesion to the substrate compared to the previous study using polymethacrylate. In addition, PNB has interesting solubility dissolution properties in the starting formulations during development of the latent image which are attributed to the helical configuration of the PNB backbone. The helical backbone is prone to ordered packing of polymer molecules in certain cases, causing dissolution rate to be largely influenced by molecular weight and additives.[15,16]

The specific PNB dielectric evaluated in this study is shown in Figure 1. This polymer is a random copolymer of a hexafluoroalcohol norbornene (NBHFA) and tert-butyl ester norbornene (NBTBE). The NBHFA is more acidic than an aliphatic primary alcohol, which provides greater dissolution characteristics in aqueous base and different reaction kinetics during the esterification cross-linking. The tert-butyl ester functionality was chosen for the protected group since the resulting carboxylic acid is required for rapid dissolution in aqueous base.[7] Since PAG is involved in both the photo-patterning and cross-linking reactions, the effect of the PAG loading was studied on photolithography and cross-linking. The tert-butyl ester to alcohol monomer ratio was studied to understand its effect on volume change during cure, modulus, hardness, CTE, and complex permittivity.

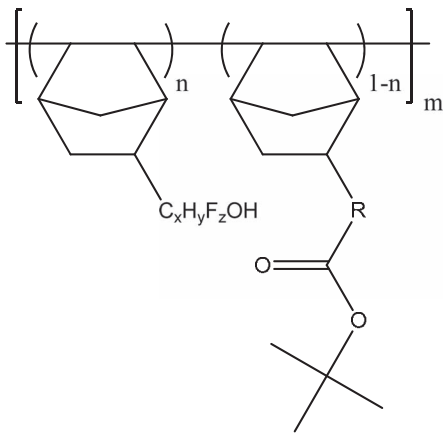

Figure 1. PNB with pendent hexafluoroalcohol and tert-butyl ester groups.

Experimental

PNB polymers were donated by Promerus, LLC (Brecksville, OH). PNB-A is a homopolymer of a NBHFA. PNB-B and PNB-C are 70:30 and 35:65 copolymers of the NBHFA and NBTBE, respectively. PNB-D is a homopolymer of NBTBE. All polymers had a weight average molecular weight of approximately 40 k g/mol. Mixtures of the four norbornene polymers were made with various loadings of PAG, 4-methylphenyl[4-(1-methylethyl)phenyl] tetrakis(pentafluorophenyl) borate (Rhodorsil FABA). The PAG was active at 248 nm radiation. To study the effect of the PAG loading, formulations 1 through 4 were prepared using PNB-C and 0.1, 0.5, 1.0, and 3.0 pphr PAG, respectively. To study the effect of monomer ratio, formulations 5 through 9 were prepared as mixtures of homopolymers and/or copolymers with 3 pphr PAG. The tested formulations are listed in Table I. Films were solvent-cast from propylene glycol monomethyl ether acetate (PGMEA) by spin-coating on <100> silicon wafers at 1500 to 3000 rpm for 60 s. The silicon wafers were treated with neat hexamethyl disilazane (HMDS) for 40 s before spin-coating to improve adhesion. The wafers were baked at 100°C for 60 s after the HMDS treatment. The PNB films were spin-coated using a CEE 100CB spin-coater. Films were baked at 140°C for 60 s to remove residual solvent and water. Samples were exposed using an Oriel Instruments flood exposure source with a 1000 W Hg(Xe) lamp filtered to 248 nm radiation. A post-exposure bake was performed at 140°C for 60 s followed by a 15 s develop in MF-319, an aqueous 0.26 N tetramethylammonium hydroxide (TMAH) solution. The film thickness was measured using a Veeco Dektak profilometer. The contrast and sensitivity of the optical exposure was measured by performing the exposures using a variable density optical mask (Opto-line International Inc.). Contrast (γ) was calculated by plotting the normalized film thickness after an aqueous base develop vs. the logarithmic exposure dose and fitting a line to the points nearest D_{100}, Equation 1. D_{100} is the lowest dose at full development and D_0 is the maximum dose where no appreciable dissolution occurred. In all cases, the insoluble-soluble transition (i.e. contrast) was sharp so that only two points could be fit and only a minimum contrast was obtained. D_{100} and D_0 were calculated by extrapolating the slope of the contrast curve to a normalized thickness of 0 and 1, respectively.

$$\gamma = \frac{1}{\log\left(D_{100}/D_0\right)} \quad [1]$$

To thermally cure the films, samples were placed in a quartz tube furnace and purged with nitrogen for 15 min at 5 LPM. The temperature was increased to 250°C over a period of 65 min and held at 250°C for 2 hr under a nitrogen flow rate of 1 LPM. Finally, the samples were cooled under nitrogen (flow rate of 1 LPM in the furnace) to room temperature. The volume change was determined by measuring the thickness before and after cure.

FTIR measurements were obtained using a Magna 560 FTIR (Nicolet Instruments). FTIR samples were coated on a KBr disk. The absorbance data was averaged over 500 scans at a resolution of 2 cm^{-1}. Mechanical properties were characterized with a Hysitron Triboindenter. Samples of approximately 2 μm thickness were indented nine times each at depths of 40 to 200 nm, which is less than 10% of the film thickness.[17] Indents were performed with a cube corner diamond tip (northstar, tip radius ~40 nm) and calibrated against

Table I. Monomer ratios for PNB formulations.

Formulation	PNB Polymers	NBHFA:NBTBE
1, 2, 3, 4	PNB-C	35:65
5	PNB-B	70:30
6	PNB-B, PNB-C	60:40
7	PNB-B, PNB-C	50:50
8	PNB-B, PNB-C	40:60
9	PNB-C, PNB-D	30:70

quartz and polycarbonate standards. The corrected tip geometry was defined by Equation 2. Step times for each indent were held constant, while the peak force was varied. The tip was loaded over a 10 s period of time, held at the peak force for 10 s to allow for time-dependent relaxations, and unloaded over a 4 s period of time.[17] Hardness, H, was calculated at the maximum load, P_{max}, divided by the projected contact area, $A(h_c)$, Equation 3. The contact area was estimated using the Oliver Pharr model in Equation 4, where h_{max} is the maximum indent depth, ε is a geometrical constant, and S is the stiffness.[18] The stiffness was defined as the initial slope of the unloading curve, and the reduced modulus was calculated using Equation 5, where β is a geometrical constant.

$$A(h_c) = 2.598h_c^2 + C_1h_c^1 + C_2h_c^{1/2} + \ldots + C_8h_c^{1/128} \quad [2]$$

$$H = \frac{P_{max}}{A(h_c)} \quad [3]$$

$$h_c = h_{max} - \frac{\varepsilon P_{max}}{S} \quad [4]$$

$$E_r = \frac{\sqrt{\pi}}{2\beta}\frac{S}{\sqrt{A(h_c)}} \quad [5]$$

$$\frac{1}{E_r} = \frac{\left(1-v_f^2\right)}{E_f} + \frac{\left(1-v_i^2\right)}{E_i} \quad [6]$$

The coefficient of thermal expansion (CTE) was measured on samples prepared on Si wafers as described above. To calculate the in-plane CTE, the radius of curvature of the sample was measured on a Flexus Tencor F2320 equipped with a temperature-controlled hotplate and a He-Ne laser. Ten measurements were taken every 10°C from 150°C to 200°C. The stress at each temperature was calculated by Stoney's equation, Equation 7, where $E_s/1\text{-}\nu_s$ is the biaxial elastic modulus of the substrate, t_s is the thickness of the substrate, t_f is the film thickness and R is the change in radius of curvature, given by Equation 8. R_1 is the radius of curvature of the bare silicon wafer, and R_2 is the radius of curvature after processing. The stress as a function of temperature was fitted with a linear least squares fit to calculate $\partial\sigma/\partial T$. Equation 9 was then used to calculate the in-plane CTE, α_{xy}, where α_s is the CTE of the substrate, and ν_f is the Poisson's ratio of the film, estimated to be 0.33.

$$\sigma = \left(\frac{E_s}{1-v_s}\right)\frac{t_s^2}{6Rt_f} \quad [7]$$

$$\frac{1}{R} = \frac{1}{R_2} - \frac{1}{R_1} \quad [8]$$

$$\frac{\partial\sigma}{\partial T} = \left(\frac{E_f}{1-v_f}\right)[\alpha_{xy} - \alpha_s] \quad [9]$$

Through-plane CTE was measured on a Woollam M-2000D ellipsometer equipped with a HCS 402 temperature-controlled stage with a liquid nitrogen pump. Ellipsometric measurements were made from 370 to 988.8 nm at an incident angle of 60 degrees. The sample was heated to 200°C and then ramped to room temperature at a rate of –5°C/min. The ellipsometric data was fit with an anisotropic model, with the in-plane and through-plane optical constants defined by Cauchy models, shown in Equation 10, where n is the refractive index, K_1, K_2, and K_3 are fitted coefficients, and λ is the wavelength. The temperature of the substrate was taken into account by modeling the Si wafer with the Si Temp JAW model. The as-collected values of polymer CTE, $\alpha_{z,measured}$, were corrected for expansion in the z-direction due to being constrained on the substrate by use of Equation 11, where α_z is the corrected through-plane CTE of the polymer. This correction accounts for the in-plane contributions to the through-plane volume change due to the constraint of the Si wafer.[19]

$$n(\lambda) = K_1 + K_2\lambda^{-2} + K_3\lambda^{-4} \quad [10]$$

$$\alpha_{z,measured} = \alpha_z + \left(\frac{2\nu_f}{1+\nu_f}\right)[\alpha_{xy} - \alpha_s] \quad [11]$$

The electrical properties of the films were measured by fabricating parallel plate capacitors. Substrates were prepared by first growing 500 nm of thermally grown SiO_2 on the silicon wafers for insulation. Aluminum was deposited by electron beam evaporation using a Kurt Lesker PVD75 to a thickness of 300 nm as measured by a quartz crystal microbalance. Films were spin-cast and cured by the same process as stated above. Aluminum was deposited on the top of the cured films by the same process. The top layer of aluminum was patterned into circular pads with a radius of 500 μm using photoresist, NR7-1500P, and the recommended processing. The photoresist pattern was transferred to the aluminum with a phosphoric acid/acetic acid/nitric acid wet etch for 210 s at room temperature. The remaining photoresist was stripped with acetone. Samples were dried at 150°C for 3 hr immediately prior to measuring the capacitance, C. Capacitance and loss tangent (tanδ) were measured at 200 kHz with a GW Instek LCR-800 on a Karl Suss probe station using a parallel RC model. The dielectric constant (i.e. real part of the complex permittivity), ε_r, was calculated by Eq. 12, where ε_o is the permittivity of free space, t is the dielectric thickness, and A is the area of the aluminum pad. The dielectric constant was corrected for fringing fields with ASTM standard D150-11 by calculating an edge capacitance, C_e, based on the approximate dielectric constant, ε_r', thickness, t, and perimeter, P.[20] The edge capacitance was then subtracted from the original capacitance, and a new dielectric constant was calculated. The imaginary, or unrecoverable portion of the permittivity is represented by tanδ, which is the tangent of the angle between the impendance vector and the negative imaginary axis on the complex impedance plane.

$$C = \frac{\varepsilon_o\varepsilon_r A}{t_f} \quad [12]$$

$$C_e = \left(0.0041\varepsilon_r' - 0.00334\ln(t) + 0.0122\right)P \quad [13]$$

Results and Discussion

Effect of PAG loading.— Acid is a catalyst for both the deprotection of the NBTBE and the esterification of NBHFA and NBTBE. The effect of the PAG loading on lithographic, mechanical and electrical properties, sensitivity, and contrast were measured for formulations 2 (0.5 pphr PAG), 3 (1.0 pphr PAG), and 4 (3.0 pphr PAG) of PNB-C (35:65 NBHFA:NBTBE). The contrast curves for these formulations are shown in Figure 2. These films were much more sensitive than common positive tone dielectric materials.[7–9] Positive tone polyimide dielectrics require 300 to 900 mJ/cm^2 to pattern due to the high concentration of DNQ needed to inhibit the dissolution of the films in aqueous base. The sensitivity and contrast of the chemically amplified PNB were found to be higher than the previously reported polymethacrylate polymer, which were 32.2 mJ/cm^2 and 5.2, respectively.[13] This is likely due to the higher acidity of the hexafluoroalcohol in the case of the PNB, which renders this polymer more readily dissolved in aqueous base developer.

It was found that increasing the PAG loading increased the sensitivity, which was expected due to the increased absorbance at 248 nm and higher photoacid concentration within the film at higher PAG loading. For all formulations, scumming was observed at doses above D_{100}, which is likely due to adsorbed water or base on the wafers before processing.[21] The hydronium cation (H_3O^+) that formed by the acid catalyst in the presence of water is less acidic than the photogenerated acid decreasing the rate of the deprotection reaction. The D_{100}

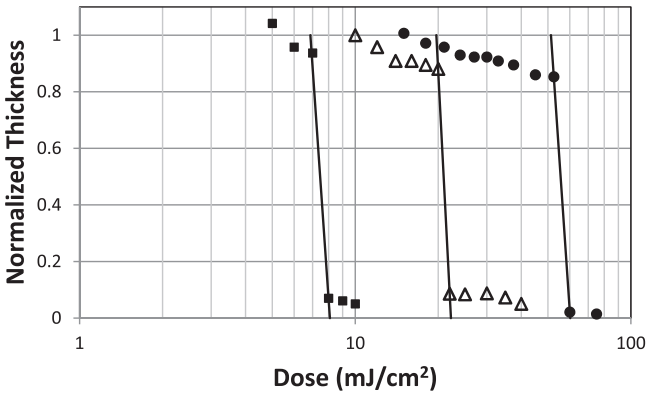

Figure 2. Contrast curves of PNB-C with 0.5 (●), 1.0 (Δ), and 3.0 (■) pphr PAG.

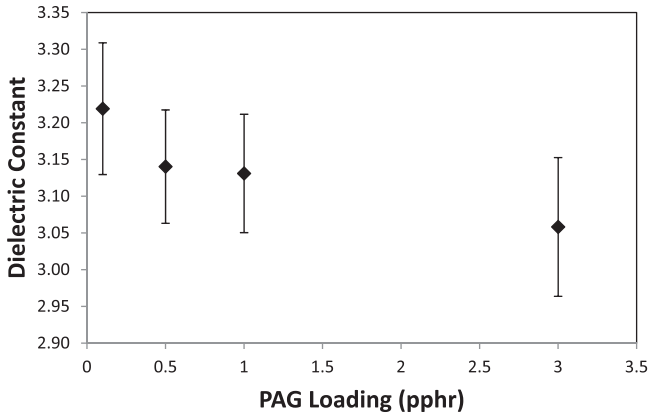

Figure 4. Dielectric constant of PNB-C as a function of PAG loading.

values for formulations 2, 3, and 4 are 60.2, 22.2, and 8.09 mJ/cm^2, respectively. The contrast was calculated with only two points. Since the contrast was high it was difficult to expose at doses which produce partial dissolution of the film. Thus, the contrast values are only minimum contrast values with the true value at least as great as the ones reported here. The calculated contrast values for 0.5, 1.0, and 3.0 pphr PAG are $\geq$ 14.3, $\geq$ 18.9, and $\geq$ 14.2, respectively. These lithographic properties show promise for the potential patterning of high aspect ratio or thick film dielectrics. Optical micrographs of patterned trenches in a 4.09 µm PNB film are shown in Figure 3. Features of 4 um half-pitch were well-resolved. Rounding of the features can be seen near the feature corners, which is a result of the high sensitivity and contrast of these PNB dielectrics. This is generally fixed by biasing the mask with dog bone features to offset the light diffracted at feature corners. The aspect ratio and feature quality are sufficient for packaging applications, and these are expected to improve with better lithographic techniques. These films were exposed in soft contact with the photomask, so diffraction under the mask limited the minimum feature size.

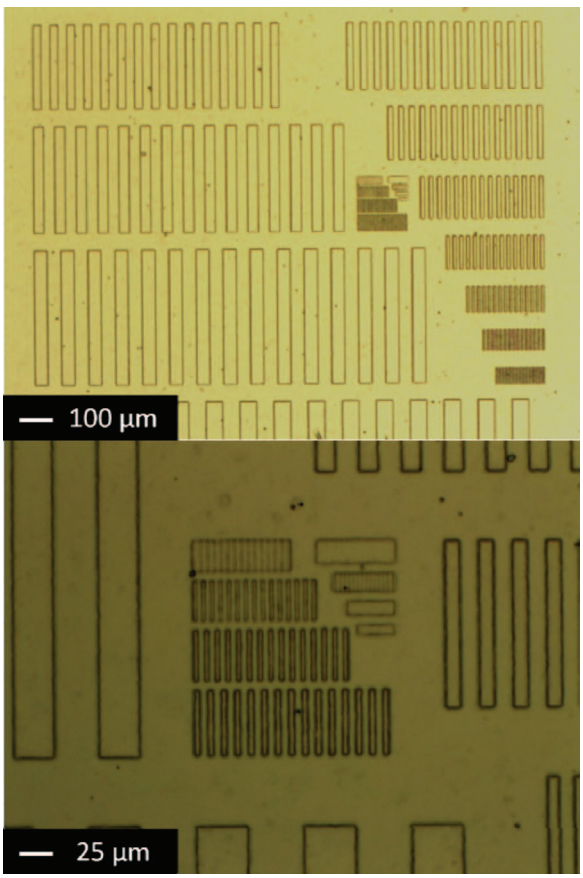

Figure 3. Optical micrograph of patterned 4.09 µm PNB film.

Modulus and hardness values were measured for formulations of PNB-C with different PAG loadings after cure by indentation. Due to the acid participation in the cross-linking reaction, it is possible that higher PAG loading would increase the reaction rate and total amount of cross-linking. This increased cross-linking could then result in higher values for the mechanical properties. However, no measurable difference was found in modulus or hardness for the films with the PAG loadings investigated here. This suggests that the films were fully cross-linked at all conditions due to the catalytic nature of the Fischer esterification cross-linking reaction. A small concentration of PAG will cause cross-linking until the film is stabilized so that mobility of functional groups is suitably inhibited. This raises the T_g of the film above the cure temperature. In addition, the non-catalyzed esterification can occur with high thermal energy, which likely occurs at the 250°C cure temperature. Thus, cross-linking can occur even with a low concentration of PAG at elevated temperature and time. The polymer films cured without PAG were found to be insoluble in PGMEA and TMAH, which is a good indication that thermal cross-linking occurred.

The complex permittivity was also measured as a function of PAG loading. The complex permittivity is comprised of the real (i.e. in-phase) and imaginary (90° out-of-phase) parts, both of which are frequency dependent. The real part of the relative permittivity is termed the dielectric constant. The imaginary, or unrecoverable loss of stored energy is reported as tanδ (i.e. ratio of the out-of-phase loss to the in-phase dielectric constant). A low dielectric constant and low tanδ are desirable for interconnect applications. Figure 4 shows the dielectric constant vs composition with one standard deviation error bars. Although the values fall within uncertainty of each other, there is a general trend of decreasing dielectric constant with increasing PAG loading. This shows that the excess PAG is not by itself making a significant contribution to the dielectric constant. Since the films are likely fully cured, it appears that the effect of the small concentration of PAG is off-set by other factors, such as the density change or esterification of polar functional groups.

Effect of monomer ratio.— The synthesis of PNB through addition polymerization allows for an easy modification of the monomer mole ratio of NBHFA to NBTBE.[22] For photopatterning, the polymer must initially be insoluble in aqueous base. A formulation with higher NBHFA with respect to NBTBE will not be inhibited because the hexafluoroalcohol, NBHFA, has an acidic proton that can dissolve in aqueous base. Further, there is likely a range of monomer ratios that are sufficiently inhibited from aqueous base solubility but still

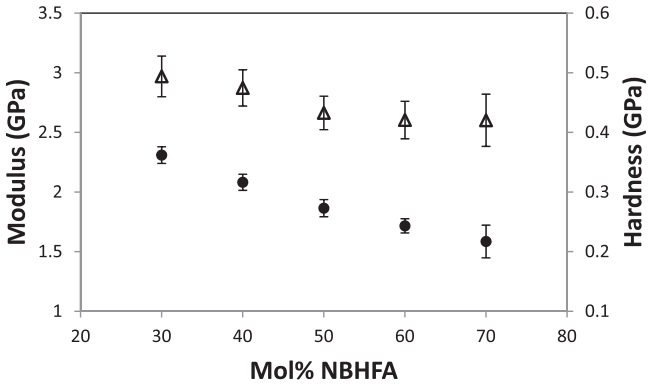

Figure 5. Elastic modulus (Δ) and hardness (●) of PNB films.

swell during the develop step. This is undesirable because swelling will distort patterned features and affect the curing reaction, yielding poor mechanical and electrical properties. Further, a polymer with an excessively high NBHFA content may require fewer NBTBE to be deprotonated to engender the solubility switch. This would likely affect the sensitivity and contrast. If the patterning required fewer deprotection reactions, this would generally lead to higher sensitivity since less time and/or radiant energy would be required. However, the resulting carboxylic acid leads to higher solubility in aqueous base, compared to NBHFA.

To measure the effect of monomer ratio in the copolymer on the properties, mixtures of the different homo- and copolymers were made. In every case, the copolymer formulations were well-mixed, and high quality films could be cast. Formulations 5 through 9 were made with varying amounts of the four PNB polymers to achieve specific monomer ratios of NBHFA to NBTBE. Each formulation had 3 pphr PAG. The reduced modulus and hardness of each formulation were measured after cure. As seen in Figure 5, both the reduced modulus and hardness increased with increasing NBTBE content. This is most likely due to the ability of the carboxylic acid formed from the NBTBE to participate in two cross-linking reactions. First, it can react with the alcohol to form the ester. Second, it can react with another carboxylic acid to form an anhydride. The formation of the anhydride was confirmed by FTIR measurements shown in Figure 6. The measurement was performed on the NBTBE homopolymer after reaction. Prior to cure, only one FTIR peak was observed in the 1850 to 1650 cm^{-1} region. The peak at 1725 cm^{-1} is due to the carbonyl stretch of NBTBE. However, it is noted that residual PGMEA may contribute to this peak slightly. After curing at 250°C for 2 hours, the original peak split into three peaks in the same spectral region. The broad peak centered at 1810 cm^{-1} is consistent with anhydride

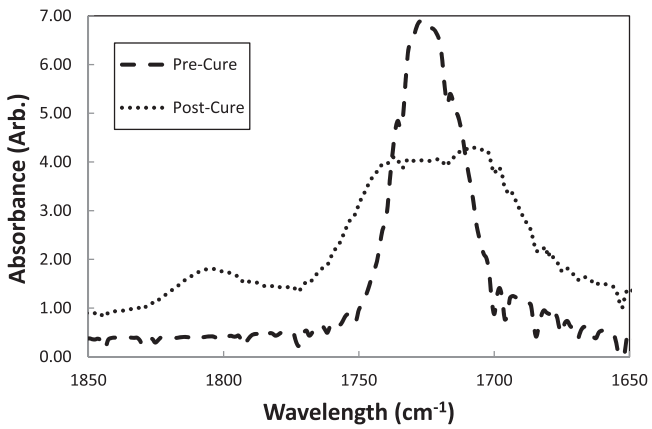

Figure 6. Anhydride peak appearance in IR after cure.

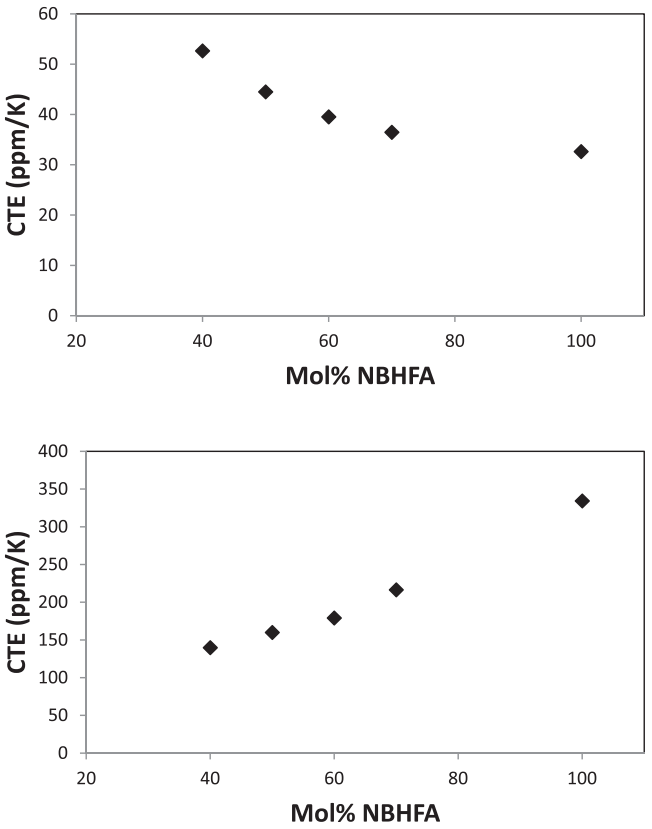

Figure 7. The CTE of PNB films measured (a) in-plane and (b) through-plane.

carbonyl stretching along with one of the peaks between 1750 and 1700 cm^{-1}. The other peak is most likely due to the carbonyl stretching of the unreacted carboxylic acid. Even though the carboxylic acid can theoretically react to completion in the NBTBE homopolymer, the mobility of the polymer chain segments decreases as the cross-linked covalent network is formed. Formation of the anhydride in the copolymers is possible, however, the ester is the rate-favored product. The same FTIR experiment was performed on a film with 30% of the NBHFA. Although a clear anhydride peak was found, the peak height was lower than the homopolymer discussed above.

Cooling the film to room temperature after curing induces a thermal strain in the polymer as a result of the mismatch in CTE between the film and the substrate. In addition, a lower Young's modulus contributes to lower stress. The in-plane and through-plane CTEs of these PNB films were measured and are shown in Figure 7. The in-plane CTE decreased with increasing NBHFA content with a value of 32.6 ppm/K for pure NBHFA homopolymer. The through-plane CTE shows the opposite trend, with a higher through-plane CTE when the NBHFA concentration increased, as shown in Figure 7b. This anisotropy can be a result of chain ordering within the polymer film. The helical conformation of PNB forms a near-linear chain which lends itself to stacking of polymer chains, especially when the PNB is functionalized with hexafluoroalcohol groups because they extensively hydrogen bond with one another resulting in in-plane orientation of the polymer along the hydrogen-bonded domains.[15] The stacked, linear assembly of the polymer is consistent with the low in-plane CTE (i.e. axial direction of the polymer backbone) because of the limited ability of the carbon-carbon bonds to expand. In the through-plane direction, the thermal expansion occurs by increasing the void space between polymer strands. When NBHFA is substituted with NBTBE, the driving force to form chain-chain ordered domains is lower because the tert-butyl ester and carboxylic acid do not form long-range hydrogen bonds like the hexafluoroalcohol. This results

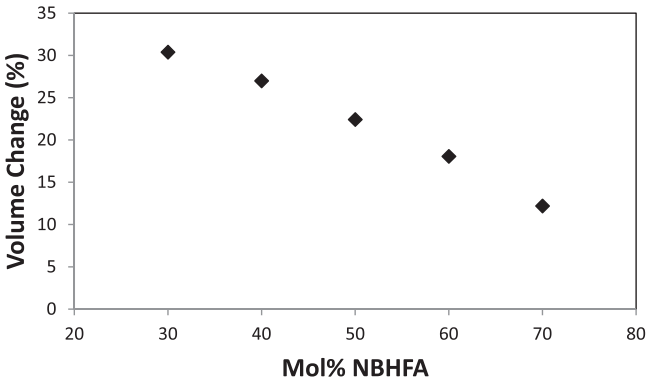

Figure 8. Volume change during thermal cure.

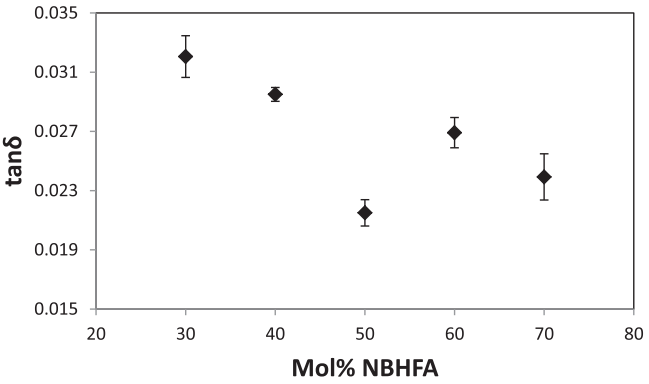

Figure 10. Tanδ of PNB films measured at 200 kHz.

in a more random configuration of the polymer strands and a more isotropic CTE.

Film shrinkage of 30% or less was observed due to mass loss and densification during the cure reactions. This also results in widening of the patterned features at the surface of the film. Two different mechanisms contribute to volume change: (i) the deprotection of the NBTBE group to form gaseous isobutylene and (ii) the formation and evolution of water by the formation of the ester or anhydride cross-links. Curing is performed at temperature greater than the boiling point of water, leading to water removal which adds to the irreversibility of the reaction. Since the film is constrained to the substrate in the in-plane dimensions, the volume change of the film is mainly reflected as a thickness decrease, as plotted in Figure 8. A decreasing mole ratio of the NBTBE monomer results in a smaller overall volume change. If the maximum cross-link density occurred at the 50:50 mole ratio, the volume change would be significantly larger for that formulation. The smallest volume change was measured for the 70 mol% NBHFA / 30 mol% NBTBE, which exhibited a change of 12.2% during cure.

The complex permittivitiy of formulations 5 through 9 were measured at 200 kHz, where the dielectric constant is reported in Figure 9 and tanδ in Figure 10. As seen in Figure 9, the dielectric constant (i.e. real part of the permittivity) decreased with increasing NBHFA content. The lowest dielectric constant was for the 70 mol% NBHFA / 30 mol% NBTBE, which had a value of 2.23. The dielectric constant at very high frequency, as measured by squaring the index of refraction determined by ellipsometry, is also plotted in Figure 9. At the higher frequency, the same 70 mol% NBHFA / 30 mol% NBTBE exhibits a value of 1.95. The trend of lower permittivity with increasing NBHFA content is confirmed by these measurements. At the high frequency used for ellipsometric measurements, dipolar and atomic contributions to the dielectric constant are not seen.[23] Current devices operate in the GHz range and will be affected by the dipolar and atomic contributions. Also important at GHz frequencies is the loss tangent (tanδ) which represents the imaginary component to the complex permittivity. Tanδ was measured for formulations 5 through 9 at 200 kHz. As with the dielectric constant, tanδ generally decreased with increasing NBHFA.

The increasing concentration of low-polarity carbon-fluorine bonds with NBHFA content contributes to lower permittivity and loss. Since the minimum dielectric constant did not occur with the 50 mol% NBHFA / 50 mol% NBTBE mixture, but rather with the 70 mol% NBHFA / 30 mol% NBTBE mixture, it appears that the contribution of the carbon-fluorine content (i.e. low polarizability and low affinity for water) outweighs the higher polarizability of the uncross-linked carboxylic acid and alcohol groups. In addition, density differences can contribute to the dielectric constant changes by adding free volume to the cured polymer film.

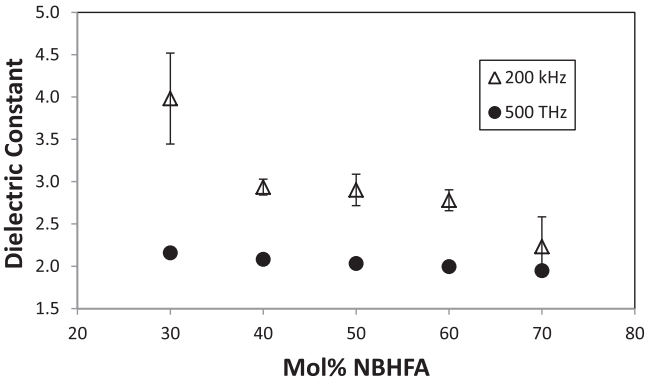

Figure 9. Dielectric constant of PNB films at 200 kHz (Δ) and 500 THz (●).

Conclusions

A positive tone, high sensitivity, low-k, dielectric has been demonstrated with PNB as a backbone material. The effect of PAG was measured. Increasing the PAG concentration up to 3 pphr was found to improve the lithographic properties, with a D_{100} of 8.09 mJ/cm^2 achieved. This sensitivity of the formulations investigated here was much higher than those of commercial dielectrics. Increasing the PAG concentration had no measurable effect on the mechanical properties or the dielectric constant. The effect of the monomer ratio was also measured. Reduced modulus and hardness were found to increase with increasing NBTBE concentration, a likely result of additional cross-linking through anhydride formation. The amount of volume shrinkage with curing and the post-cure dielectric constant and tanδ decreased by reducing the NBTBE concentration. For formulation 5 (70% NBHFA / 30% NBTBE), the volume shrinkage was 12.2% and the permittivity was 2.23. These values are promising for this material's use as a photo-definable, permanent, low-k dielectric.

Acknowledgments

The authors gratefully acknowledge Promerus, LLC for providing PNB materials and for technical discussions.

References

1. R. R. Tummala and M. Swaminathan, *Introduction to System-on-Package*. (McGraw-Hill, 2008).
2. G. Maier, *Prog. Polym. Sci.* **26**, 3 (2001).
3. P. A. Kohl, *Annu. Rev. Chem. Biomol. Eng.* **2**, 379 (2011).
4. M. Raeis-Zadeh, E. Elce, B. Knapp, and P. A. Kohl, *J. Appl. Polym. Sci.* **120**, 1916 (2011).
5. V. Rajarathinam, C. H. Lightsey, T. Osborn, B. Knapp, E. Elce, S. A. Bidstrup Allen, and P. A. Kohl, *J. Electron. Mater.* **38**, 778 (2009).
6. *Assembly and Packaging*. International Tecnology Roadmap for Semiconductors (2010).
7. B. K. Mueller, E. Elce, A. M. Grillo, and P. A. Kohl, *J. Appl. Polym. Sci.* **127**, 4653 (2012).

8. Y. So, E. J. Stark, L. Yongfu, S. Kisting, A. Achen, K. Baranek, D. Scheck, J. Hetzner, J. J. Fokenroth, M. Topper, and T. Baumgartner, *IEEE Trans. Adv. Packag.* **29**, 741 (2006).
9. X. Z. Jin and H. Ishii, *J. Appl. Polym. Sci.* **98**, 15 (2005).
10. C. A. Mack, *Appl. Opt.* **27**, 4913 (1988).
11. S. A. Macdonald, H. Ito, and C. G. Willson, *Microelectron. Eng.* **1**, 269 (1985).
12. E. Reichmanis, F. M. Houlihan, O. Nalamasu, and T. X. Neenan, *Chem. Mater.* **3**, 394 (1991).
13. B. K. Mueller and P. A. Kohl, *J. Appl. Polym. Sci.* **130**, 759 (2013).
14. M. Huang, O. G. Yeow, C. Y. Poo, and T. Jiang, *IEEE Trans. Components, Packag. Manuf. Technol.* **31**, 767 (2008).
15. W. J. Chung, C. L. Henderson, and P. J. Ludovice, *Macromol. Theory Simulations* **19**, 421 (2010).
16. T. Hoskins, W. J. Chung, A. Agrawal, P. J. Ludovice, and C. L. Henderson, *Macromolecules* **37**, 4512 (2004).
17. B. J. Briscoe, L. Fiori, and E. Pelillo, *J. Phys. D Appl. Phys* **31**, 2395 (1998).
18. W. C. Oliver and G. M. Pharr, *J. Mater. Res.* **7**, 1564 (1992).
19. J. E. Pye and C. B. Roth, *Macromolecules* **46**, 9455 (2013).
20. *D150-11 Standard Test Methods for AC Loss Characteristics and Permittivity (Dielectric Constant) of Solid Electrical Insulation*. 1–20.
21. S. A. MacDonald, N. J. Clecak, H. R. Wendt, C. G. Willson, C. D. Snyder, C. J. Knors, N. B. Deyoe, J. G. Maltabes, J. R. Morrow, A. E. McGuire, and S. J. Holmes, *Proc. SPIE* **1466**, 2 (1991).
22. U. Okoroanyanwu, T. Shimokawa, J. Byers, and C. G. Willson, *Chem. Mater.* **10**, 3319 (1998).
23. J. O. Simpson and A. K. St. Clair, *Thin Solid Films* **308-309**, 480 (1997).